University of Tartu

Faculty of Science and Technology

Institute of Technology

Yigit Orhan

Rapid Ice Cube Production with 3D Printed Copper Moulds

Master's Thesis (30 ECTS)

Material Science and Technology

Supervisor:

Alvo Aabloo

Tartu 2022

ABSTRACT In English

The aim of the work was to design a device for making ice to be placed in cocktails. The technical precondition was that it was not possible to have an ice storage facility, and the number and quantity of ice cubes had to be checked very carefully, also the formation time for an ice cube is nearly 10 seconds. With this solution, the ice accumulation bucket is totally removed which means a compact unit for YANU.

CERCS: P190 thermodynamics, computer aided design, optimization, finite element method

Keywords: beverage serving robots, thermodynamics, additive manufacturing, computation, refrigeration

ABSTRACT in Estonian

Töö eesmärgiks oli koostada kokteilidesse paigutatava jää valmistamise seade. Tehniliseks eeltingimuseks oli, et jää hoidlat ei ole võimalik omada, samuti tuleb jääkuubikute arvu ja kogust väga täpselt kontrollida. Jääkuubiku valmimisaeg peab olema väiksem kui 10 sekundit. Selle lahendusega loobutakse jäähoidlast täielikult.

CERCS: P190 termodünaamika, arvutipõhine disain, optimeerimine, lõplike elementide meetod

Keywords: joogi serveerimise robotid, termodünaamika

Table of Contents

Symbols & Abbreviations

Symbol	Description	Unit
ρ	Density	$[kg/m^3]$
C_p	Specific Heat at constant pressure	$[J/kg°C]$
v	Velocity vector	$[m/s]\ x, y, z$
∇T	Temperature gradient in space [x, y, z axis]	$[°C/m]$
q	Conductive heat flux	$[W/m^2]$
β	Bulk expansion coefficient	$[°C^{-1}]$
t	Time	$[s]$
∇p	Pressure gradient in space	$[Pa]$
τ	Viscous stress tensor	$[N/m^2]$
∇v	Velocity gradient in space (acceleration)	$[m/s^2]$
Q	Heat source per unit volume	$[W/m^3]$
k	Thermal conductivity	$[W/mC°]$
θ	Porosity / Volume ratio	[%]
L	Latent heat fusion	$[kJ/kg]$
α_m	Thermal diffusivity	$[m^2/s]$
δ	Boundary layer thickness	$[m]$
h	Convection coefficient	$[W/m^2°C]$
Re	Reynolds number	-
Pr	Prandtl number	-
Nu	Nusselt number	-
Bi	Biot number	-
μ	Dynamic viscosity	$[N.s/m^2]$

Table 1. Abbreviations

1.INTRODUCTION

Food and beverage serving robots might have the place to replace bartender in mass service cases and it is trendy in the global market in order to develop smart devices with the integration of AI and software. The market for robot developers and foodservice industries is quite competitive and the battle gets intensified more and more. While updating serving robots with a considerable pace, it sorts out essential troubles like precision serving without overpours, but in the meantime, they cause negative influences on humans in terms of employment shortage and also technical failures of units mounted on devices such as ice machines, peristaltic pumps or moving elements exceeding the range of motion.

Food serving robots are widely being used at restaurants in United States, and the main purpose of them is to develop a business in terms of serving speed and getting rid of the typical issues created by human staff. For instance, Flippy[1] is one of the mightiest robots which is able in flipping burgers and preparing French fries. As well as the food serving robots, the number of manufactured beverage-serving robots shows a massive climb, especially post-pandemic. The main positive aspects of developing drink serving robots is to get rid of conversations with drunk clients, maximize the serving efficiency and accuracy of the system and to minimize the liquid waste.

In thesis, distinct engineering approaches are clarified in order to ramp up ice production rate considering energy-saving and cost effective ways.

1

1.1 ROBOT BARTENDERS: Why?

In this section, I give a short analysis of what positive sides and disadvantages robot bartenders have, compared to human bartenders.

AUTOMATION BENEFITS

In automated systems, there are no shift times, sickness, or annual leave and it brings up the opportunity to produce without any lack of speed. The increase in production at a lower cost produces significant benefits for manufacturers. The initial investment cost of automated systems is predictably high; however, it can be recovered in a relatively short time and the gains from that point onwards are exponential.

CONSISTENCY

Human precision launches from the maximum level at the very beginning of a day, however, over time lack of concentration inevitably occurs and this is what causes some sort of deficit in quality level. It is impossible to compare humans to machines. Robots are able to be operated as long as the commands are on. Hereby, showing the same level of performance, in the long run, called consistency or sustainability, is the key spot for manufacturers.

INCREASING FUNCTIONALITY

The functionality of smart machines was restricted to the heavy payload in transportation equipment manufacturing. Nevertheless, with the increasing functionality of robots, for instance, the food processing industry is adopting automation with considerably low payload robots. Segments like the food and beverage industry are minimizing human contact in the production process in order to run health authority standards.

NO DISCUSSION WITH ROBOTS

There is a saying that “Problems are likely to appear where people are”. Basically, minimizing the quantity of staff in a workplace benefit in terms of no existence of any debate or disagreements among workers and employers. On the other hand, talking with a drunk client is one of the main duties of a bartender. Even possible clients might like to get laid with a bartender. Thereby, with robots, there will be fewer problems for sure rather than a situation without robots.

AUTOMATION NEGATIVE SIDES

Besides many innovations in AI technology, some weaknesses should be considered as well. The most outstanding point is the unemployment issue which might be a major threat. Beverage serving machines replace human work which means that instead of human bartenders, robots grab this task from them. It might cause financial issues.

Furthermore, robots are coded according to what they are supposed to do by software and control engineers, however, they are not able to perform if something is out of program boundaries. They can illustrate weird output and are likely to break down easily. At this point, reliability is also something no one can ignore. Building robotic components, as well as the repairing process, require a large amount of financial power. There are numerous sensitive parts and sensors which have to be produced in high precision which means higher costs. All those high maintenance and manufacturing costs put their customers' budgets into trouble.

1.2 CURRENT STATE OF ART IN BARTENDER SOLUTIONS

Here I give an overview of some well-known competitive food and beverage serving machines in the market.

CECILIA

Cecilia[2] is a beverage serving machine that is designed for providing a drinking service for customers. It is able to serve 120 drinks per hour. The machine can be operated in various countries due to its qualification in 40 languages. Customers can order their drinks by not only speaking but also using the smart screen located on the front side. The payment method has many alternatives such as cashless payment, ID scanner, or dashboard buttons. Versatile mechanical arms can perform sophisticated movements like shaking and stirring. It is programmed based on mixing a precise volume of ingredients, thereby the benefit of that particular talent is to reduce food waste.

Figure 1. The front panel of Cecilia

2

MILK-IT

Milk-it is a patented milk tap solution designed for the hospitality and foodservice industry. The principle of this automated device is to minimize milk consumption by at least 8%, which saves a considerable amount of money. To explain more technically is that a large package of milk is assembled to an electric tap which implements an easy replacement or reloading ability and an efficient work environment indeed. It presents eco-friendly ideas for the global market. It saves about 4 seconds in serving time per coffee cup and allows the user to serve more cups when demand is high. Milk-it[3] is an automated innovation that is not only ramping up productivity but also managing hygiene issues easily. It has a daily special cleaning program that keeps the device operating at the top levels of hygiene.

ACUR-C (Autonomous Clear Up Robot Type C)

The device is developed and manufactured by Smile Robotics for picking dish plates from tables, it does the same mission as the staff at a restaurant does. Operation launches by the time it receives a command via smart Pad screen. It is equipped with one mechanical arm with a gripper that is truly able to lift dish plates gently in order to minimize the tipping over risk. If the gripper assembly is taken into hand in detail, it is seen that it consists of two pieces of sheet metal that have sufficient length with the aim of lifting the plate in balance.

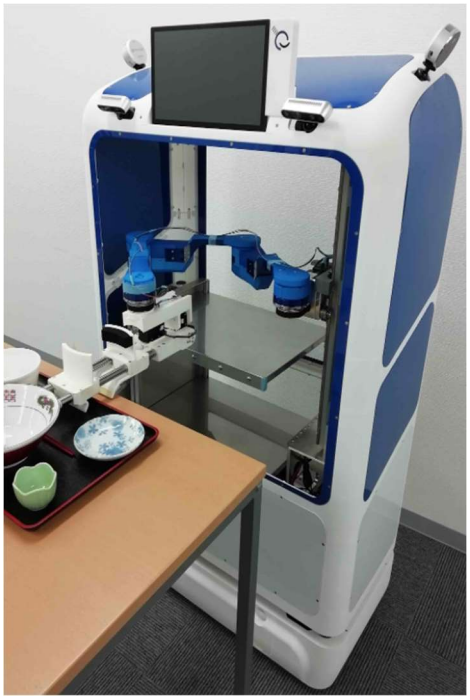

Figure 2. ACUR-C

3

The mechanical arm can collect dishes at a 1-meter distance from the table and there is no specific restriction on the degree of freedom. In the chassis, numerous shelves are built which allow her to put multiple plates. 2 laser sensors and 4 high-tech cameras create an ability to detect all the surroundings at about 360°. By this configuration, the collision risk is kept pretty low.

Shell structure which is impossible to be touched from the outside is fixed on the base frame for safety. The complexity of components is kept as low as possible and that benefits ease of implementation and maintenance.

Makr Shakr - TONI COMPATTO

TONI is an innovative drink servicing robot that is the most competitive one in the market. What makes it mighty is its serving speed of about 50 drinks per hour. The device has one mechanical arm which can perform complicated movements including mixing and shaking. Customers order drinks from the Makr Shakr[4] application via mobile and tablets. It can prepare hot and cold beverages also with alcoholic and non-alcoholic alternatives.

Figure 3. Manufactured by Makr Shakr, Toni Compatto

YANU Robotic Pub

The YANU robotic bar, has a fully autonomous operating system that serves drinks to customers with the latest artificial intelligence technology. It was manufactured by an Estonian-based company. The mechanism is not only dazzling looking with decorative design and concept but also captures high technology components, such as sensors and control units in its boundaries. Especially on these critical days, when all over the world is suffering from the pandemic, people would prefer to avoid physical contact with another person. It is the right time slot in which the YANU can make its way in the market.

4

Outside geometry looks inspired by a smooth cylinder which attracts the people. Machine powered by artificial intelligence can receive card and mobile payments on its application. It is not only to serve a drink to the client but also capable of communicating with the client about her best beverage choice and performing unique jokes which creates a kind interaction with clients.

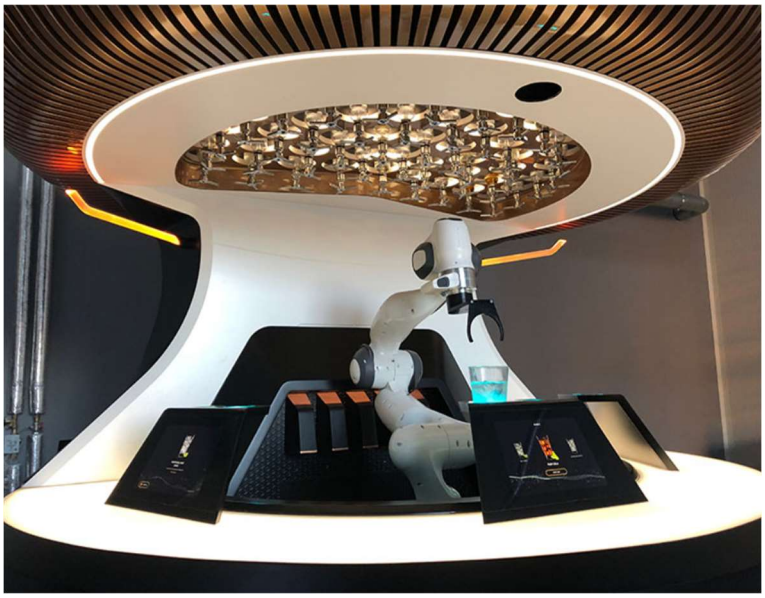

Figure 4. Footage of YANU

In a single load, YANU[5] is equipped to prepare 1500 cocktails and has a peak capacity of serving 100 drinks in an hour. That pace illustrates how demanding this device is among the rival bartenders. The main reason why people improved this kind of machine is based on several needs in the global market. High staff turnover rate, descending performance by a human bartender in a day, and of course immediate need for a contactless solution due to the pandemic.

Without the help of engineering design tools, it seems difficult to build the whole assembly at all. Technically, the engineering team utilizes computer-aided design software called Solid Edge to render a full mock-up of the device. Particularly what modules in software are exploited for YANU can be defined as, sheet metal designing, additive manufacturing techniques (3D Printing), data management, Keyshot engine which enables engineers to visualize the moving parts in one image, and electrical routing which allows a platform to design cable, wire connections beforehand. These modules stated above would gain the assembling team a vast amount of time during the mounting process.

5

Robot	(TONI Veloce) Makr-Shakr	Yanu	Acur-C	Cecilia	Milk-it
Size [cm]	355x284x263	295x245x200	135x77x43	243x60x50	37x15x20
No of Drinks per hour	120	100	-	120	3 liter/min
Soft drinks	+	+	-	-	-
Bottle Capacity on holder	158	45	-	-	10 liter-milk bag
Bubbled drinks	+	+	-	-	-
coffee	+	+	-	-	-
milk	-	-	-	-	+
multimedia	+	+	+	+	-
Alcoholic	+	+	-	+	-
(A)Assembled on site or (U)Delivered as a unit?	A	A	U	A	U
Estimated no of drinks served with one load	2500-3000	1000-1500	-	-	-
Units on market	-	2000	-	-	2000
Company value	18M$	3M$	-	-	1.5M$
Year of	2014	2016	2019	2021	2014

Table 2. Comparison table of most competitive bartender robots

2. MOTIVATION OF RESEARCH AND HYPOTHESIS

In this work, an ice machine setup for Yanu was proposed alongside understanding the working principle of the beverage serving system, a special need appears regarding ice machines. The typical ice machines existing on the market are not suitable for Yanu solution. To make it clearer, not only the ice forming speed but also being able to dispense ice cubes equally per drink seems to be the main points that should be overhauled.

2.1 Challenges

Automation

Commonly drink serving devices should distribute ice precisely into glasses as part of their mission. Typical machines in the market have a system that chilled water flowing from up to down and attaching the frost mould surface and gradually the very first ice layers begin to form a thin crystallization on the surface. Once the desired thickness is reached, it takes a short heat impulse called defrosting.

In order to put a requested amount of ice in a beverage, an automated counting procedure is used. This can be achieved by a screw mechanism that pulls cubes in its grooves to transmit them from the bucket to the ice outlet. It is complex to set quantity due to nonuniform geometry.

2.2 Motivation of Development

The main target of my work is to find an innovative solution to ramp up ice cube production speed from a cost-effective and energy-saving point of view. The work will try to solve the problem like being in an unpleasant position due to the failure of ice machines as we are the creator of them. To achieve the desired results, we utilize material science and thermodynamic fundamentals as well as fluid dynamics, computer-aided design software, metal 3D printing technology, measurement & testing techniques, and heat transfer finite element method.

2.3 TECHNICAL REQUIREMENTS OF A NEW MACHINE

Use Case Description

As shown in Figure 5, the robot receives an order for a drink that may or may not involve ice, and if yes, this is the signal to start forming ice. Meanwhile, Yanu's smart arm picks the empty glass from the glass holder which takes 8 to 10 seconds. Tap water (~10°C) is injected into the frozen mould by a pump. Copper mould has cavities for enough ice in one drink. Estimated ice forming time varies from 10 to 15 seconds which is massively dependent on parameters like cavity volume, the initial temperature of the mould, ice cube wall thickness etc.

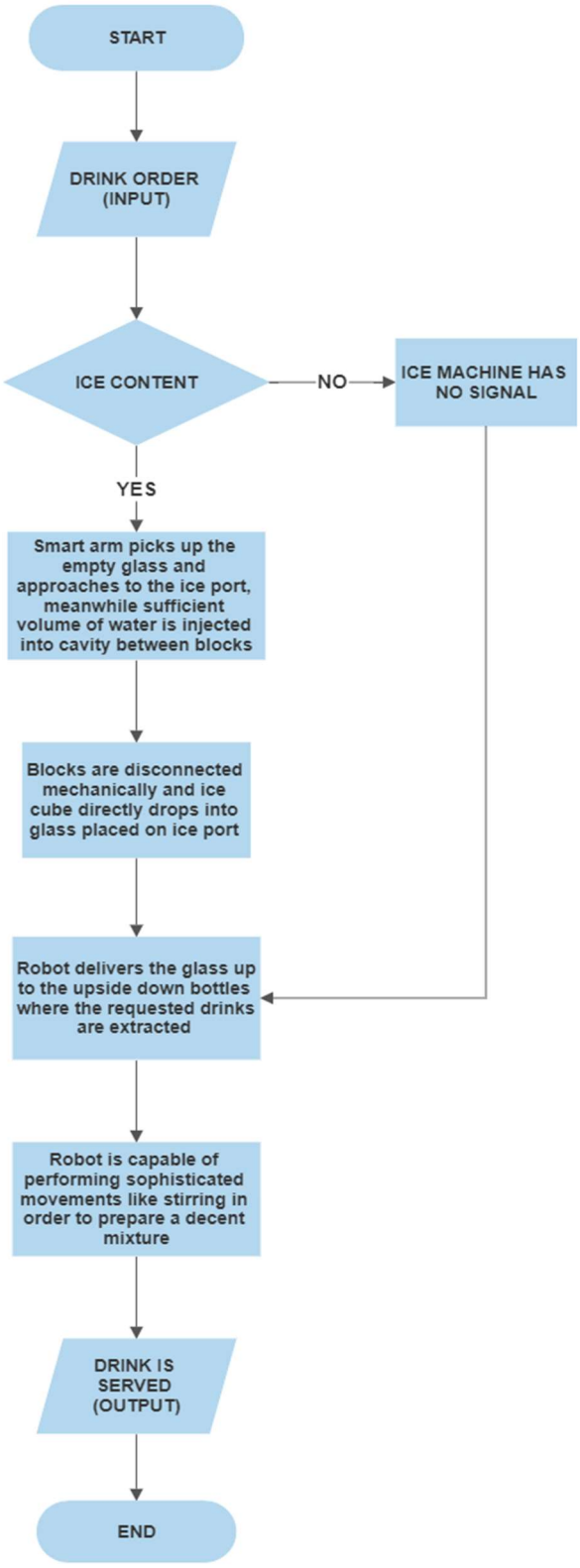

Figure 5. Use Case Diagram

3. METHODOLOGY

3.1 The design

According to my design, ice has to be formed within 10 to 15 seconds and to achieve that the optimum wall thickness is tested to be around 3 mm, whereas outer dimensions are pretty variable according to the glass size, of course, the bigger ice volume means longer survival time in the drink. Ice cubes are formed in metal 3D Printed blocks which are made of copper due to their excellent thermal conductivity. Conformal cooling channels are designed in a mould block which is the same cooling system that is being used for plastic injection moulding applications.

The reason why the wall thickness is specified as 3 mm, is expressed in the practical and computational section of the paper.

The problems I tried to solve with new solutions were as follows

- Ice bucket removal
- Dispersing an equal amount of ice is sorted out by instantaneous crystallization

What components are added to build a new solution

- 3D Printed copper blocks with conformal cooling channels
- A mechanical system that enables blocks to open and close repetitively
- Ethylene Glycol aqueous solution is circulated for keeping the moulds at -20°C
- Circulation pump

Draft Angle Estimation

The geometry which has an inward draft angle provides ease in the evacuation of ice out of the mould. As seen on Figure 6, negative and positive draft angles are demonstrated. In case a part has an outward draft angle like Part C, evacuating the part out of the mould is impossible unless the block is made of more than one part.

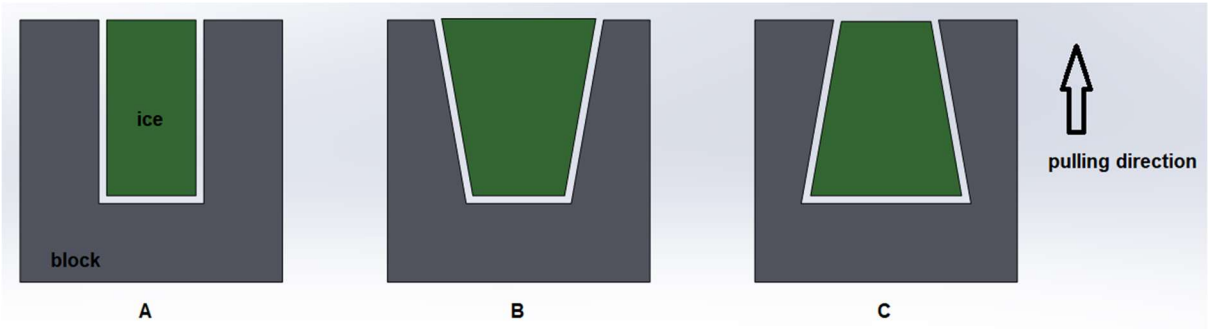

Figure 6. A (challenging 0°), B (Ideal 10° Overcut), C (Bad 10° Undercut)

Various Ice Cube & Mould Design Concepts

Distinct design concepts are seen in Figure 7. Change in block volume and surface area determines exactly how fast they can cool down. If the cooling performance is considered, the optimization is necessary which is to minimize the block volume and maximize the block surface area as denoted in Equation 2. Secondly, a larger volume means heavier the block, which means more energy is required to cool down as formula seen at Equation 1. My preference is to pick the first design from the left-hand side as shown in Figure 7. The main reason for that is, having lower L_C values among the three.

The characteristic length is the significant parameter in the cooling speed of the block. Lower L_c values bring faster cooling capability.

$$Q = \rho V C_P \Delta T \quad [joule] \quad (1)$$

$$L_c = \frac{V}{A_S} \quad [m] \quad (2)$$

$$Parameters$$

$$V = Block\ volume$$

$$A_S = Block\ surface\ area$$

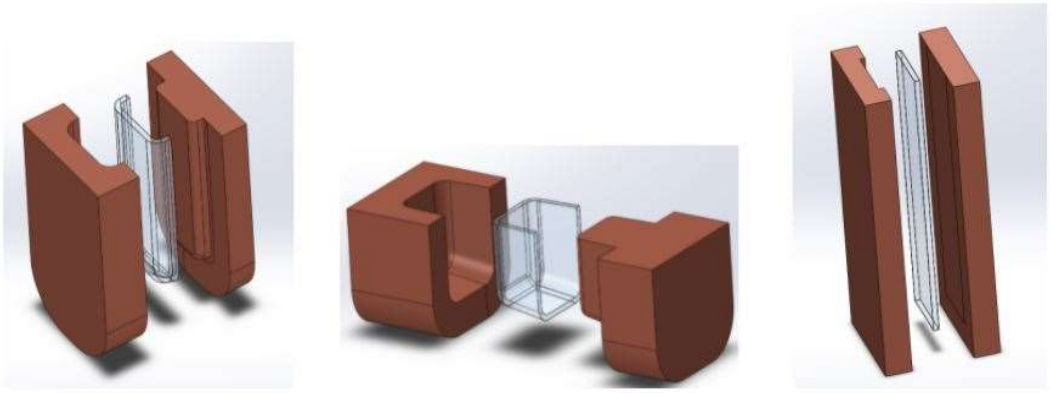

Figure 7. Various Ice Cube & Mould Design Concepts

3.2 Full Description of the New Design

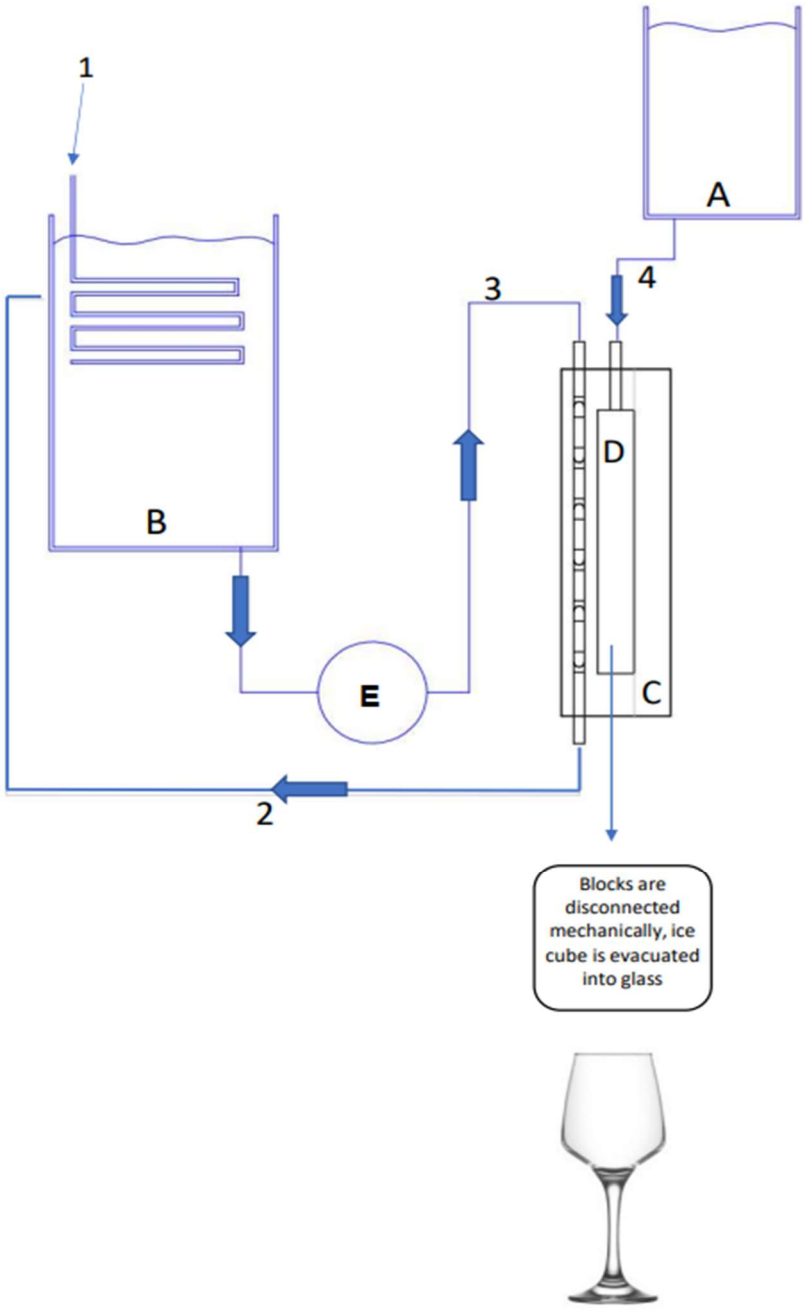

Figure 8. Schematic view of the New Design [A-Water Tank, B-Coolant Reservoir, C-Metal Printed Copper Blocks, D-Cavity, E-Circulation Pump, L1-Evaporator Coils, L2-Coolant Drainage, L3-Pressurised Coolant, L4-Water Inlet]

Evaporator coils are placed in the reservoir to keep the liquid temperature constant and in most systems, R134-A (tetrafluoromethane) is being pushed through coils in the refrigeration industry. 3D Printed blocks made of copper involve 2 pieces: a core and a tool. Ice is formed in the cavity between blocks. The surface quality of the cavity is a vital parameter to get a smoother ice cube. The circulation pump plays an ultimate role in cooling performance due to

adjusting the flow velocity. For Line 4, because of the inviscid characteristic of water molecules, an advanced pump is not required. For instance, a peristaltic pump or the valve mechanism would be a suitable way to push water into the cavity.

Not all volumes of the cavity could be filled with the water as ice density is lower than the water density. During the freezing, the structure expands. The maximum allowable volume of water is *0.92 x total volume of the cavity*. Otherwise, overpoured water might be frozen through Line 4 which causes a blockage for the next cycle.

3.3 Thermodynamic Model

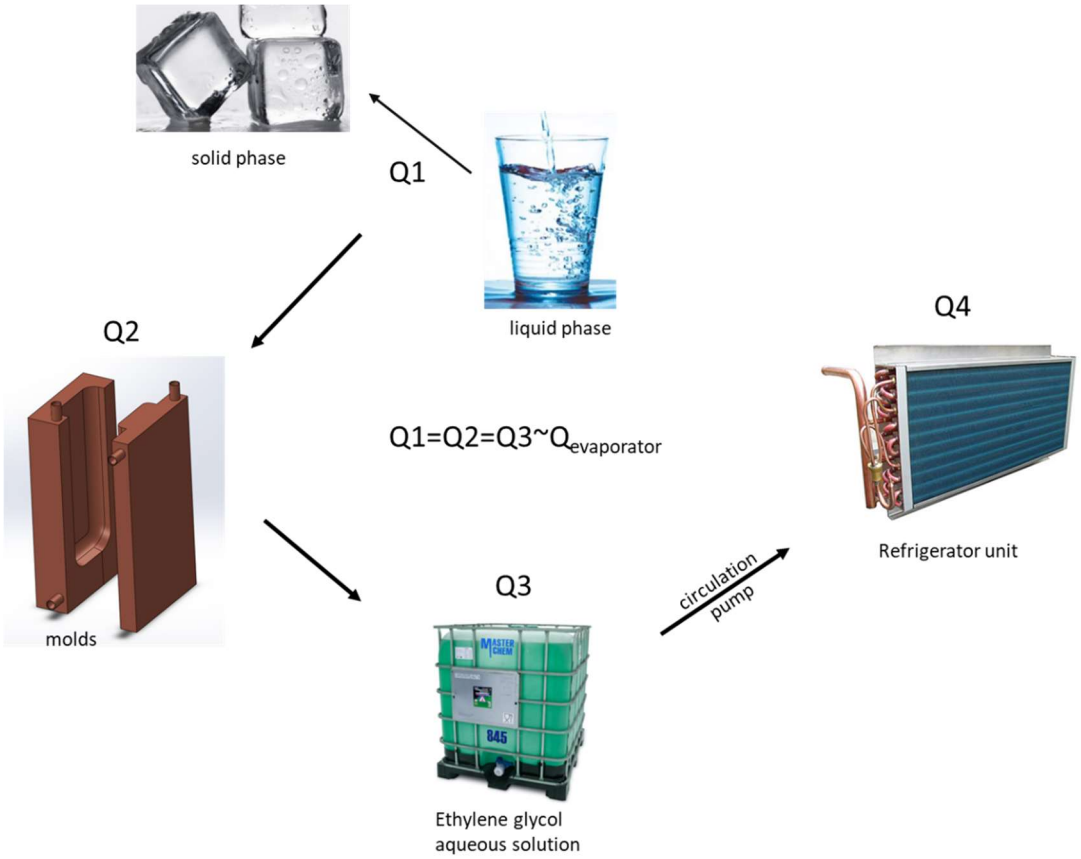

Figure 9. Stakeholders of the Energy Flow Model

3.4 Modeling

According to Figure 9, I describe energy equations for each part.

Water cooling and freezing energy model

All three phases which are liquid, transition, and solid are modelled in the following equations and total energy is specified in Equation 6. Mass of the system is preserved at all correlations.

$$q_{water} = m_{liquid} * C_{\rho(water)} * \Delta T_1 \quad (3) \qquad \Delta T_1 = T_{water} - T_{freezing\ point}$$

$$q_{phase} = m_{liquid/solid} * \Delta L \quad (4) \qquad \Delta L = 334\ [kJ/kg]$$

$$q_{solid} = m_{solid} * C_{\rho(ice)} * \Delta T_2 \quad (5) \qquad \Delta T_2 = T_{freezing\ point} - T_{ice}$$

$$Q_1 = q_{liquid} + q_{phase} + q_{solid} \quad (6)$$

Mould Energy Model

It is assumed that the system has no energy loss, therefore energy drawn from water has to be fully transmitted to metal blocks as seen on following correlations. As a result of forming an ice cube through the cavity, a temperature rise is likely seen on blocks.

$$Q_1 = Q_2$$

$$Q_2 = \rho_{block} * V_{block} * C_{p(block)} * \Delta T_3 \quad (7)$$

$$\Delta T_3 = T_{block\ post\ ice\ forming} - T_{block\ before\ ice\ forming}$$

Cooling Fluid Energy Model

A circulation pump forces the cooling fluid through channels which are designed in block geometry to cool the block down to its initial temperature with the purpose of getting prepared for the next cycle. Heat transfer that occurred in this section is not quite as simple as before despite forced convection correlations which are described in detail under the cooling performance title. Furthermore, with the disregard of energy loss, the blocks conduct the entire energy to the cooling liquid.

$$Q_2 = Q_3$$

Refrigerator Energy Model (evaporator unit)

Heat absorbed by the evaporator coils has to be decent to keep the cooling liquid temperature at a constant level in the specified cycle time. An enthalpy-pressure diagram of refrigerant, defined in Figure 11, is necessary to evaluate the amount of heat, $Q_{evaporator}$, which the evaporator sucks from the environment.

$$Q_3 = Q_4$$

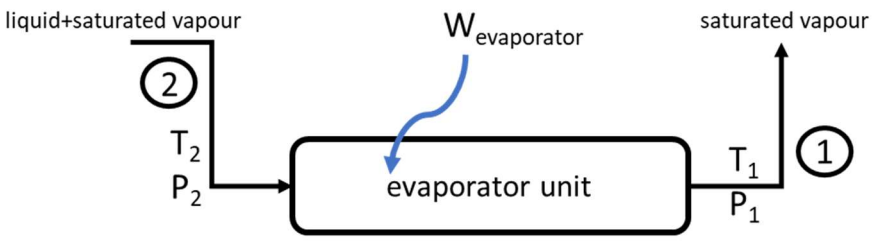

Figure 10. Evaporator Scheme

$T_2(inlet\ temp.), P_2(inlet\ pressure), T_1(outlet\ temp.), P_1(outlet\ pressure)$

The reservoir is filled with cooling fluid, and evaporator coils are positioned inside the tank which absorb heat from the fluid. In the refrigeration industry, plenty of refrigerants have been used on-demand such as R134A (tetrafluoromethane), R22, R404A, R717 (ammonia), and R744 (carbon dioxide). In my system R134a[6] was used.

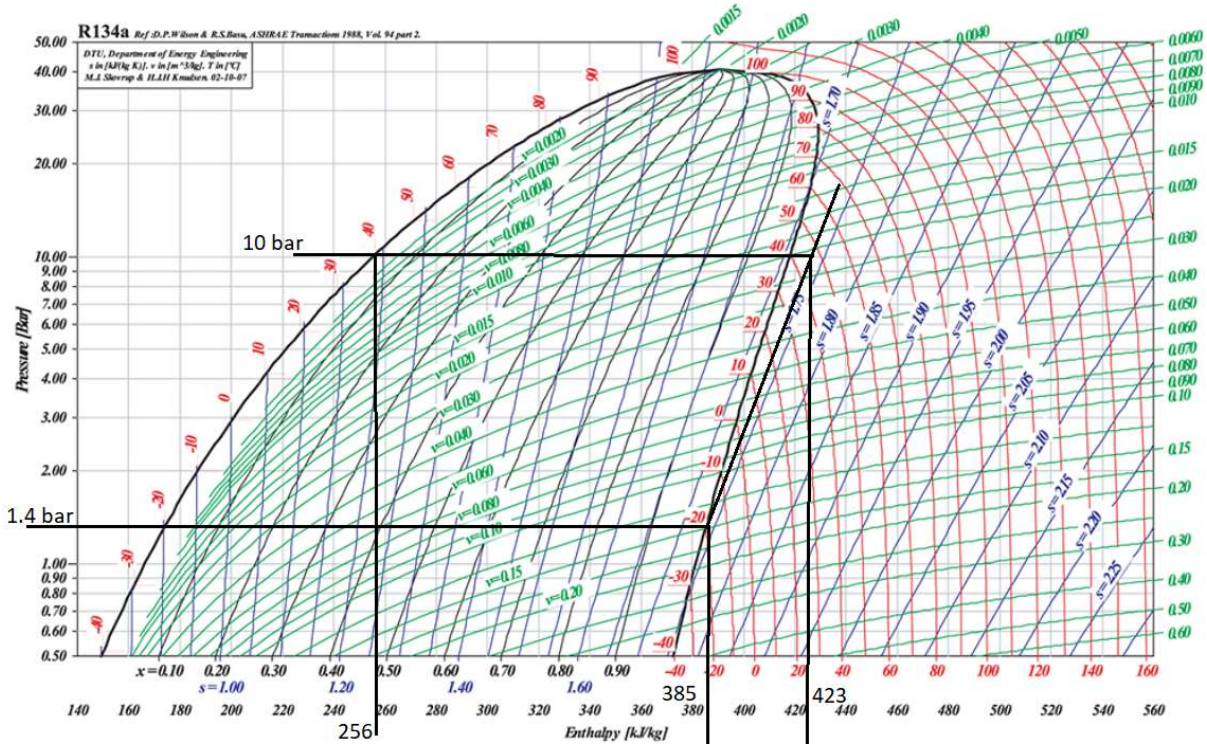

Figure 11. Enthalpy-Pressure Chart for refrigerant R134A

Port 1 (Evaporator Outlet) & Port 2 (Evaporator Inlet)

For the outlet port, the only one phase is observed as saturated vapour which has remarkably low temperature values. As seen in Figure 10, Port 1 goes all the way through the compressor for boosting the refrigerator pressure and temperature.

Inside the inlet port, we see the liquid-vapour mix is extracted from the expansion valve whose function is to drop the pressure massively in order to reach frost degrees. The coolant is formed as a mixture of liquid and saturated vapour. Volume fraction of phases can be detected from the enthalpy-pressure chart. For the evaporator unit, isobaric and isothermal considerations are

6

assumed (P_2=P_1 & T_2=T_1), due to the fact that pressure drop and temperature change inside the evaporator unit are low, which might be neglected.

Evaporator Power [W] or [BTUh]

The flow velocity of coolant (kinetic energy change) and elevation change (potential energy change) between other elements are ignorable. No moving parts are driven in this unit which means no shaft work (seen only in the compressor) at all. Therefore, the evaporator model[7] looks like below.

$$\Delta H + \Delta E_{kinetic} + \Delta E_{potential} = W_{evaporator} - W_{shaft} \quad (energy\ model)$$
$$\Delta H = H_1 - H_2 \quad (8)$$

$$W_{evaporator} = \Delta H_{internal\ energy}\ [Joule]$$
$$Q_{evaporator} = \dot{m} * \Delta H\ [Watt] \quad (9)$$

$$Parameters\ ;$$
$$\dot{m}_{R134A} = mass\ flow\ rate\ [kg/s]$$
$$H_1 = enthalpy\ outlet\ [kj/kg]$$
$$H_2 = enthalpy\ inlet [kj/kg]$$

Ice formation

The shape of the cavity is the key player to successfully form ice fast. The mission is to optimize the ice wall thickness with regards to maximizing the survival time in a drink and also forming it as quickly as possible. At super low wall thicknesses, it has demonstrated a poor resistivity against melting, and by contrast, at thick wall thicknesses, the mould temperature has to see at least -60 °C to achieve it within ~10 seconds. The phase transition time is directly proportional to the second power of thickness value. The limiting factor is heat transfer as shown in the following integration.

7

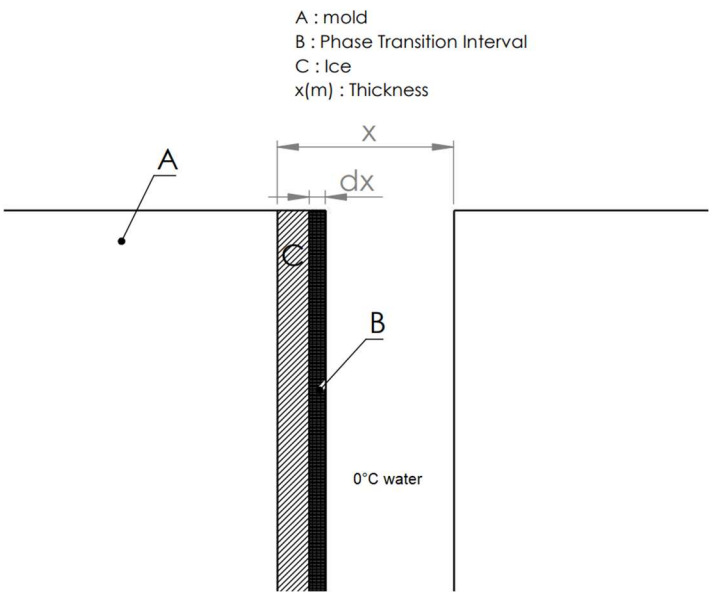

Figure 12. Scheme illustrates the water-ice transition

Launching from the Equation 10, which refers to the general heat conduction model, relevant substitutions are demonstrated from Equation 10 to Equation 13.

$$\frac{dQ}{dt} = \frac{k * A_S * \Delta T}{x} \quad (10)$$

$$dQ = dm * \Delta L \quad (11)$$

$$dm = \rho * A_S * dx \quad (12)$$

$$dQ = \rho * A_S * dx * \Delta L \quad (13)$$

Surface area term on both sides is simplified at Equation 14;

$$\frac{\rho * A_S * dx * \Delta L}{dt} = \frac{k * A_S * \Delta T}{x} \quad (14)$$

$$\int_0^x x\,dx = \int_0^t \frac{k * \Delta T}{\rho * \Delta L} dt \quad (15)$$

Post integration method the correlation between the time and ice thickness is stated at Equation 16.

$$t = \frac{\rho * \Delta L * x^2}{2 * k * \Delta T}\ [s] \quad (16)$$

Parameters

$\rho_{ice} = density\ [kg/m^3]$ — $dm = mass\ of\ differential\ part\ [kg]$

$k_{ice} = heat\ conductivity [\ W/m.C°]$ — $dx = thickness\ of\ differential\ part\ [m]$

$A_S = surface\ area\ [m^2]$

$\Delta L = latent\ heat\ fusion\ [J/kg]$

$t = elapsed\ time\ [s]$

$\frac{dQ}{dt} = heat\ flow\ rate\ [J/s]$

$T_{phase\ change} = 0°C\ (water/ice)$

$x_{ice} = wall\ thickness\ [m]$

$\Delta T = T_{phase\ change} - T_{mould}\ [C°]$

3.5 Heat Transfer with the Phase Change Combination

Temperature Model

The equation below is iterated for the phase change physics of water, from liquid to solid. According to the first law of thermodynamics, for a non-uniform isotropic environment the general temperature equation, created by partial differentials is stated as follows, regarding that mass and radiation transfer is assumed to be zero.

$$\underbrace{\rho C_P \frac{\partial T}{\partial t}}_{\text{Change in temperature by time}} + \underbrace{\rho C_P v.\nabla T}_{\text{Change in temperature in space by flow}} = \underbrace{-\nabla.q}_{\text{net heat flux}} + \underbrace{\beta T\left(\frac{\partial p}{\partial t} + v.\nabla p\right)}_{\text{Pressure work term}} + \underbrace{\tau : \nabla v}_{\text{Viscous heating}} + \underbrace{Q}_{\text{heat source}} \qquad (17)$$

In my model, since the velocity field resulting from density variations during the phase change is very low. Because of that, the element called temperature gradient in space by flow has disappeared. Moreover, instead of gases, considerations are done for fluids which have highly incompressible structure. Minor changes in pressure are observed. As a result of that, pressure work term is neglected. Lastly, in most of the hydraulic systems viscous heating effect has to be taken into account, although, for my model not. At the end of the simplifications the equation looks smooth as follows.

$$\rho C_P \frac{\partial T}{\partial t} + \nabla.q = Q \qquad (18)$$

To define the conduction heat flux vector shown as “q”, Fourier’s Law correlation is used as follows. The parameter k describes the thermal conductivity.

$$q = -k\nabla T \qquad (19)$$

In case Equation 19 is substituted in Equation 18, we get the final part below.

$$\rho C_P \frac{\partial T}{\partial t} + \nabla(-k\nabla T) = Q \qquad (20)$$

Phase Change Interference Model

Here, the combination of temperature model and phase change physics is taken on hand in detail. In principle the equation is the same, despite the fact that, rather than a single phase, 2 phases survive in this section. Phase 1 refers to water and Phase 2 is ice state. Most of the physical values between phases illustrate a variation. For instance, during the water to ice phase change the density drops down resulting in volume expansion. There is a series of correlation to evaluate effective values, such as $C_{eq}, \rho_{eq}, k_{eq}$. The main equation is fully defined in Equation 21.

$$\rho_{eq} C_{eq} \frac{\partial T}{\partial t} + \nabla(-k_{eq} \nabla T) = Q \qquad (21)$$

The effective mass density is calculated by using the, θ ,which is defined as porosity or volume fraction of phases seen in Equation 22.

$$\rho_{eq} = \theta \rho_{phase1} + (1 - \theta) \rho_{phase2} \qquad (22)$$

The effective thermal conductivity can be modelled by using the same method described in Equation 23.

$$k_{eq} = \theta k_{phase1} + (1 - \theta) k_{phase2} \qquad (23)$$

The effective specific heat at constant pressure depends on multiple parameters such as latent heat (L), volume fraction, effective mass density and thermal diffusivity (α_m) modelled as follows.

$$C_{eq} = \frac{1}{\rho_{eq}} \left(\theta \rho_{phase1} C_{p,phase1} + (1 - \theta) \rho_{phase2} C_{p,phase2}\right) + L \frac{\partial \alpha_m}{\partial T} \qquad (24)$$

$$\alpha_m = 0.5 \frac{(1 - \theta) \rho_{phase2} - \theta \rho_{phase1}}{\theta \rho_{phase1} + (1 - \theta) \rho_{phase2}} \qquad (25)$$

3.6 Cooling Performance and Elapsed Time

In order to evaluate the cooling coefficient of a mould block, there are thermodynamic parameters one following another, those are figured out respectively. They are expressed as follows.

Cooling Channel Geometry

Channel profile is designed as circular. Increasing the profile perimeter allows heat transfer enhancement which means a phenomenal rate of convection. The fabrication method is

Selective Laser Melting in my thesis. Designing a simpler geometry like a circular profiled tube is more reasonable in terms of manufacturability.

Reynolds Number for Internal Forced Flow, Re

The Reynolds number needs to be calculated. The scale is defined in Table 3. Fluid flow is streamlined and defined as laminar at low velocity, jumps up to turbulence at high velocity. However, in between transitional flow cannot be ignored which carries both laminar and turbulent flow behavior inside. Reynolds number is evaluated with different formulas with regards to the environment such as external or internal forced conditions. Here, my model for internal forced circumstances is defined in Equation 26.

$$Re = \frac{\rho V_m D_h}{\mu} \qquad (26)$$

$Re < 2300$	*laminar flow*
$2300 \leq Re \leq 10000$	*transitional flow*
$Re > 10000$	*turbulent flow*

Table 3. Flow type determination

$$Parameters;$$
$$\rho = fluid\ density\ [kg/m^3]$$
$$V_m = mean\ velocity\ [m/s]$$
$$D_h = hydraulic\ diameter\ [m]$$
$$\mu = dynamic\ viscosity\ [Pa.s]$$

Prandtl Number, Pr

It is a dimensionless number that can be defined as the ratio of kinematic viscosity to thermal diffusivity. Prandtl number travels at low values for inviscid fluids, whereas, ramps up for viscid fluids. Each fluid has its Prandtl value according to chemical structure and molecular interaction forces as seen in Table 4. At -20°C my coolant's Prandtl number is 209.

$$Pr = \frac{momentum\ diffusivity}{thermal\ diffusivity} = \frac{\mu/\rho}{k/(C_p\rho)} = \frac{C_p\mu}{k} \qquad (27)$$

$$Parameters;$$
$$C_p = Specific\ Heat\ at\ constant\ pressure\ [J/kg°C]$$
$$\mu = Dynamic\ viscosity\ [Pa.s]$$
$$k = Heat\ conductivity\ [W/m°C]$$

Fluid	Pr
Liquid metals	*0.004-0.030*
Gases	*0.7-1.0*
Water	*1.7-13.7*
Light Organic Fluids	*5-50*
Oils	*50-100,000*
Glycerin	*2000-100,000*

Table 4. Pr comparison between different fluids

Thermal Entry Length, L_t

Fluid has a uniform temperature at the tube inlet and for this consideration particles in the layer have a contact with the surface of the tube which is assumed surface temperature. Surface temperature is modeled higher than the fluid temperature. This is the launching point of convection heat transfer and the development of the thermal boundary layer along the tube. The thermal boundary layer thickness is shown with the symbol δ_r. $T_{(r)}$ drops towards the centerline of the tube because the fluid is being heated.
The region where the flow is both hydrodynamically and thermally developed has stable velocity and temperature profiles. It is called a fully developed flow. Calculations which have been made for fully developed flow give engineers a more radical perspective.

Fully developed phase remarks that the change of $(T_s - T)/(T_s - T_m)$ with respect to the x-axis equals zero, seen in Equation 28.

$$\frac{\partial}{\partial x}\left[\frac{T_S(x) - T(r,x)}{T_S(x) - T_m(x)}\right] = 0 \quad (28)$$

$$L_{t,laminar} = 0.05RePrD_h \quad (29)$$

symbols;

$T(r,x) = temperature\ at\ given\ coordinates$

$T_s = surface\ temperature$

$T_m = mean\ fluid\ temperature$

In all cases the fluid is able to reach the hydrodynamically developed point quicker than the thermally developed point. The main reason of that is, convection coefficient takes much longer to become constant than the friction factor.

Nusselt Number Thermal Entry Region Correlation

At standard conditions the Nusselt number[8] equals 3.66 in a thermally fully developed condition. However, if the thermal entry length is by far higher than the total length of the tube, the Nusselt number is expected to be higher than 3.66 which can be modelled in Equation 30.

$$L_t >> total\ channel\ length\ ;\ [m]$$

$$Nu = 3.66 + \frac{0.065(D_h/L)RePr}{1 + 0.04[(D_h/L)RePr]^{2/3}} \quad (30)$$

Convection Coefficient, h

In thermal engineering, convection is the definition which indicates heat transfer occurring in fluids. This can form either natural or forced environments. To clarify the forced convection, fluid is forced by a fan or pump to circulate the system with the aim of absorbing or delivering the heat. For enclosure and external natural convection, fluid has no remarkable velocity, however, change in temperature in fluid particles causes density variations which triggers the buoyancy natural effect. The molecules which are heated have become less dense. By natural behavior of physics, buoyancy forces have lifted those less dense particles to the top and meanwhile cooler particles have been pushed down due to its relatively heavier structure.
The relation between Nusselt number and convection coefficient is expressed below in Equation 31.

$$h = \frac{kNu}{D_h}\ [W/m^{2\circ}C] \quad (31)$$

Fluid Exit Temperature Evaluation

In the heat exchanger, fluid exit temperature can be derived from the following equations beginning from Equation 32.

$$\dot{m}C_p dT_{(x)} = h\left(T_s - T_{(x)}\right)dA_s \quad (32)$$

$$dA_s = Pdx \quad (33)$$

$$dT_{(x)} = -d(T_s - T_{(x)}) \quad (34)$$

If Eq. 34 and Eq. 33 are integrated in Eq. 32, then we get the equation below.

8

$$\frac{d(T_s - T_{(x)})}{T_s - T_{(x)}} = -\frac{hP}{\dot{m}C_p}dx \quad \Rightarrow ln\frac{T_s - T_e}{T_s - T_i} = -\frac{hA_s}{\dot{m}C_p} \quad \{x = 0\ (tube\ inlet), \quad T_{(0)} = T_i\}$$

$$\{x = L\ (tube\ outlet), T_{(L)} = T_e\}$$

In short, fluid exit temperature model looks as follows,

$$T_e = T_s - (T_s - T_i)exp(-hA_s/\dot{m}C_p) \quad [°C] \qquad (35)$$

$$Parameters;$$
$$dA_s = differential\ surface\ area$$
$$dx = differential\ length$$
$$P = perimeter\ of\ channel\ profile$$
$$T_e = fluid\ exit\ temperature$$
$$T_{(x)} = fluid\ temperature\ at\ any\ x\ location$$
$$T_i = fluid\ inlet\ temperature$$
$$T_s = block\ surface\ temperature\ \ (variable\ parameter)$$

Maximum Cooling Power

The moment when the ice cube is taken off, is defined as maximum heat transfer rate. In spite of the fact that, the biggest delta between the fluid and block surface temperature is formed exactly in this time slot. The essential heat flow rate function is emphasized at Equation 36.

$$Q_{(t)} = \dot{m} * C_{p,fluid} * \left(T_{(t)} - T_i\right) \quad [W] \quad (36) \quad heat\ rejected\ with\ respect\ to\ time$$

The rate of Q demonstrates an exponential decline, due to the fact that, ΔT gets smaller by time, in the meantime mass flow rate and specific heat capacity are constant. If the ice removal time is considered to be zero, the maximum cooling power is modelled in Equation 37.

$$t = 0 \ \rightarrow \ Q_{(0)} = Q_{max} \quad (37)$$

Mould Temperature Model with Respect to Time

Biot Number Criteria, *Bi*

While a metal block is being cooled by the surrounding fluid, heat is ejected first by convection and afterwards conduction within the block. The Biot number is the ratio of internal resistance of the block to the external resistance of the block. The model is prescribed as follows.

$$Bi = \frac{h * L_C}{k} \qquad (38)$$

Lumped system analysis is used widely by engineers to estimate the instant temperature of a solid. However, there is a criterion about that. In case of $Bi \leq 0.1$, lumped system analysis is applicable which means the temperature profile in a solid body is distributed uniformly. On the other hand, $Bi > 0.1$ declares that temperature variations within the block are quite high, thereby, the more sophisticated correlation is needed.

Time Constant, b

Time constant depends on particular parameters like the block geometry, specific heat capacity, block density and convection coefficient which is defined at Equation 39. The larger b value means the faster cooling or heating ability.

$$b = \frac{h}{\rho_{BLOCK} * C_{P,BLOCK} * L_C} \ [1/s] \qquad (39)$$

The block temperature at random time in terms of second, $T(t)$, is modelled at Equation 40.

$$\frac{T(t) - T_\infty}{T_i - T_\infty} = e^{-bt} \quad \rightarrow \quad T(t) = T_\infty + (T_i - T_\infty)e^{-bt} \ [°C] \qquad (40)$$

Wall Friction Factor, f

When the flow is at laminar state, the friction factor does not depend on wall surface roughness. This algorithm does show a different response when it switches to a turbulent state. The only influencing parameter for this state is Reynolds magnitude. Friction factors on different aspect ratios are specified at Table 5.

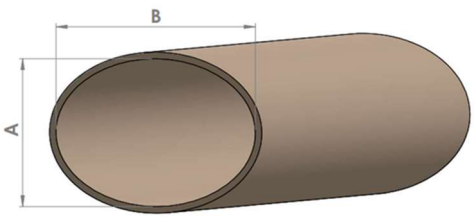

Figure 13. Channel Sketch

B/A	f
1	$64.00/Re$
2	$67.28/Re$
4	$72.96/Re$
8	$76.60/Re$
16	$78.16/Re$

Table 5. Friction factors according to geometry

For other cases, where the wall roughness has to be taken into account, a chart called Moody Diagram[9] as seen on Figure 14, presents a wide range of friction factors to be modelled in fluid mechanics.

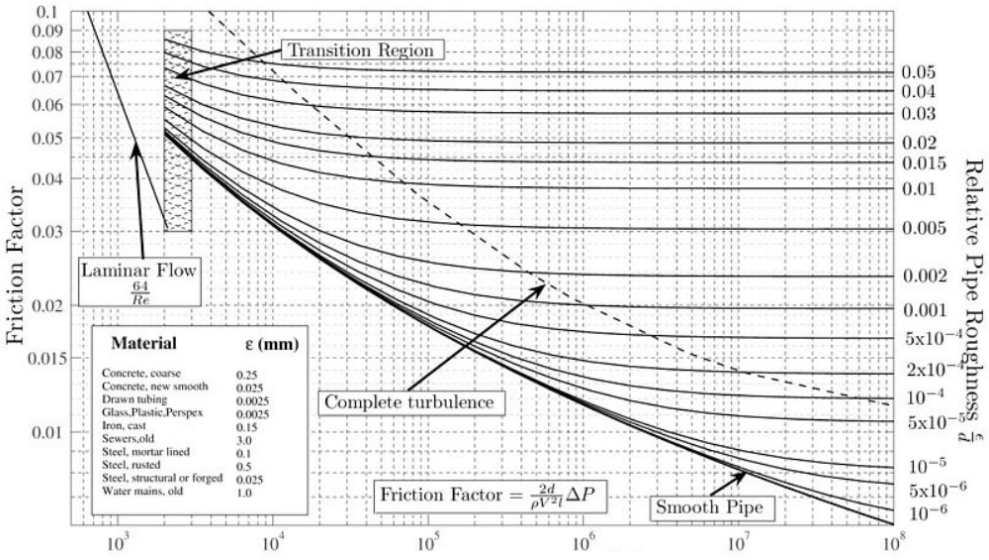

Figure 14. Moody Diagram

Pressure Model Through Channel, P

It is expected to see the pressure drop between inlet and outlet of the channel due to the frictional forces. The model stated at Equation 41 is valid for both laminar and turbulent flow, however, only for fully developed flow.

$$\Delta P = 0.5 f \frac{L}{D_h} \rho {V_m}^2 \quad [Pa] \qquad (41)$$

9

Circulation Pump Requirement

The cooling fluids have a viscous structure which applies a lot of pressure onto pumps. But also channel geometrical parameters play an important role here. To achieve the circulation, the minimum pump power model is stated as follows.

$$\dot{W}_{pump} = (\dot{m}\Delta P)/\rho \quad [Watt] \qquad (42)$$

Cooling Fluid

Ethylene glycol and water forms a homogeneous solution which is widely being used for heat transfer applications in which temperature drops below 0°C. The solvent has protected inner tubes and coils from possible corrosion forming. Rather than ethylene glycol, propylene glycol also serves a variety of cooling applications as well.

Solvation of Ethylene Glycol

$$HO - CH_2CH_2 - OH$$

The pure ethylene glycol has a higher freezing point, -12°C than a 50% aqueous solution, -40°C. Therefore, mixing the base glycol with water gives lower freezing point to the solvent. Moreover, parameters like specific heat, thermal conductivity, mass density and dynamic viscosity depend on concentration and temperature of solution as seen in Table 6.

%Volume in mixture (Monoethylene glycol)	Temperature[° C]	Density [kg/m^3]	Specific Heat $[kJ/kg.K]$	Thermal Conductivity $[W/m.K]$	Dynamic Viscosity $x10^{-3}[N.s/m^2]$
52	-40	1108	3.04	0.416	110.80
	-20	**1100**	**3.11**	**0.409**	**27.50**
	0	1092	3.19	0.405	10.37
	20	1082	3.26	0.402	4.87
	40	1069	3.34	0.398	2.57
	60	1057	3.41	0.394	1.59
	80	1045	3.49	0.390	1.05
	100	1032	3.56	0.385	0.722

Table 6. Properties of ethylene glycol aqueous solution

3.7 MEASUREMENTS

Experimental Layout

Two aluminum blocks and 3 mm aluminum 5754 sheet metal are jammed together with a clamp as depicted in Figure 16. The mechanism is placed in a circular metal can and soaked into -36°C refrigerant liquid to cool down. 2 pieces of K Type thermocouple are attached on appropriate spots.

Figure 15. Lab refrigerator

One overhangs inside a 3 mm cavity and the other has direct contact with the block. Therefore, the first thermocouple delivers temperature data in the cavity which belongs to water/ice and the second one does demonstrate instant mould temperature. Some amount of tap water is sucked in a 5 ml syringe and stored in the household fridge to cool down. As the can floats in the coolant bath, the block temperature shows a gradually descending profile, however, approximately 45 minutes later it becomes stable at a point, -20°C.

Figure 16. Blocks are clamped together for testing

Water syringe is taken out from the refrigerator and injected into the cavity. Injection process is carried out rapid, about ~1 second. Meanwhile, temperature gradients of both water/ice and mould are recorded on the software called NI LabView[10].

K-Type Thermal Sensors

K type thermocouples can be used in most environmental conditions such as in the water or dry air, because wires are made of nickel-based material which gives them a brilliant corrosion

10

resistance. It is composed of a non-magnetic positive wire called Chromel and a magnetic negative wire called Alumel. In the experiment, I have used an Exposed Junction[11] type which refers to a thermocouple having a soldered naked wire tip. The beauty of utilizing exposed junction type is to possess the fastest response time, about 0.2 seconds. With this practical work, I have gained experience in soldering.

Calibration of K-Type Thermocouples

It is necessary to calibrate thermocouples. The calibration procedure is highlighted as follows.

Step 1; To make proper calibration of the thermocouple, I used two reference values. One is ice bath which is at 0°C.

Step 2; The other is done with the help of a cryostat. The cryostat is equipped with a calibrated PT-100[12] temperature sensor inside cooling reservoir. Its measuring principle is to determine temperature by resistance change, 0.385Ω/ºC. The sensor has been calibrated every 6 months repetitively.

The cryostat has a reservoir with the evaporator coils attached inside wall. The reservoir is filled with the cooling fluid, ethylene glycol aqueous solution. The cooling fluid temperature is set at -36°C. 0°C refers to 1.24 millivolts as performed in an ice bath and -36°C refers to 1.06 millivolts. As a result of linearization, it is revealed that each 1°C change in temperature matters 0.005 millivolts in potential.

Monitoring the Temperature Data

A digital output created by a sensor can be transmitted to a computer system directly, by contrast, analog sensor equipment called Data Acquisition Module (DAQ) is necessary as shown in Figure 17.

Figure 17. A footage of the NI DAQ module, USB-6009 DAQ

11
12

It receives the analogue signal as input and converts it to a digitized output. *AD-8495* voltage amplifiers were used as viewed in Figure 18.

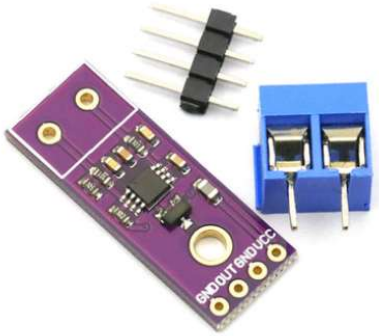

Figure 18. AD-8495 K type Amplifier

Circuit Diagram

An amplifier has 4 ports on one side and 2 ports on the other side. To start with 2 port-side, these junctions are for positive and negative wires routing from a thermocouple. The other 4 port-side has been specified as the following. VCC is the short form of Voltage Common Collector which is the power input, 5V. GND is the short form of Ground. OUT is the short form of Analogue Output which reflects the data and is linked to the Al 0+ port on DAQ. If more than one amplifier is used, the other's OUT ports should be linked to either Al 1+, Al 2+, or Al 3+ spots. As viewed in Figure 19, all stations on DAQ are labeled with the numbers. The diagram is plotted to enlighten the stated explanations above.

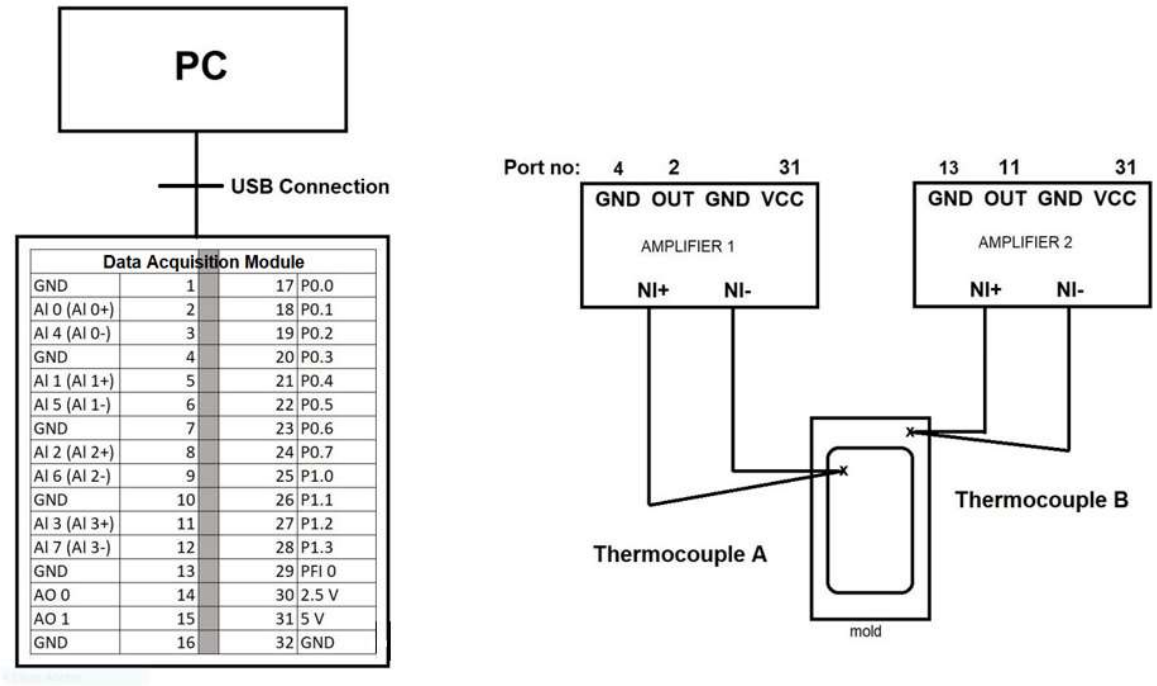

Figure 19. DAQ Connection Diagram

List of Components Used In Experimental Work

1. Cryostat[13]
LAUDA Proline RP 1845

2. Ethylene Glycol[14] 50% aqueous solution bath

3. Mould construction (3mm aluminum sheet metal clamped between aluminum cubic blocks)

4. Syringe for water injection

5. A metal can

6. K type thermocouples, AD-8495 amplifier, USB 6009 DAQ Module, PC

Error Analysis

The environment conditions such as humidity, air temperature where the experiment was carried out have to be considered. Otherwise, results may lead a fault at the end of the day. While the experiment was being performed, the place had a standard room temperature of 22 °C which was measured by a calibrated thermometer. Therefore, the metal moulds gain heat from surroundings by radiation as they are not thermally insulated. Secondly, the canister was placed at the bottom of coolant bath. The coolant level covers only half of the canister height, in that sense, the moulds inside the can have no direct contact with the coolant. As the air is quite poor at conductivity, which hinders heat transfer. Due to the reasons stated above, even though the coolant temperature is set to -36°C on the indicator, I could only see -20°C on the mould wall as the lowest.

4.RESULTS

In this section I clarified and compared experimental and computational outcomes.

4.1 Experimental Outcome

$Parameters$	Liquid phase	Transition	Solid phase
$Temperature\ (°C)$	$8 \rightarrow 0$	~ 0	$0 \rightarrow -T$
$Elapsed\ time(s)$	1.5	12	$depends\ on - T$

13
14

Table 7. Defines output parameters
"T" value is assumed to be 5

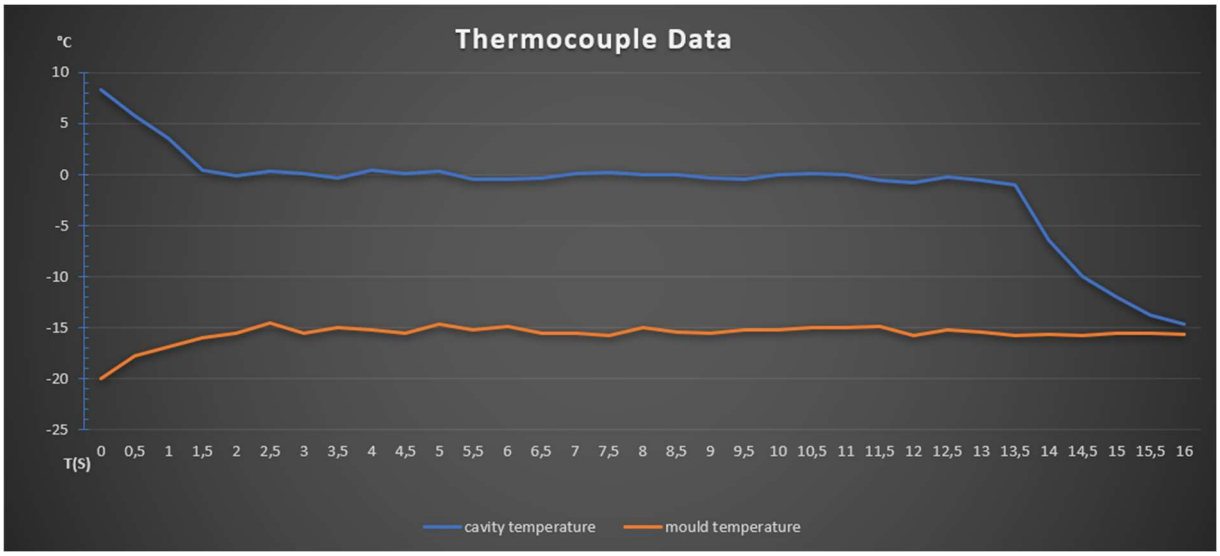

Figure 20. The image demonstrates experimental temperature data on both cavity and mould block

As a result of the experiment, for 3 mm cavity, it took 13,5 seconds to get fully ice with the 8°C and -20°C initial temperatures of the water and the mould block respectively. At the end of the measuring process, the temperature of the mould block rose 5°C.

4.2 Modeling & Computational Results

Crystallization Time [s]

The computational freezing analysis is done for variable thicknesses by using COMSOL Multiphysics[15]. The phase transition module was exploited. As described in Figure 21, the area in blue and white indicates mould (made from copper) and cavity (filled with water) respectively. An appropriate mesh on the model was set. The free triangular mesh is assigned with denser distribution on cavity walls due to the contact zone where the heat transfer begins. The initial conditions are specified in Table 8. The scale parameters regarding mesh are enlightened in Table 9.

15

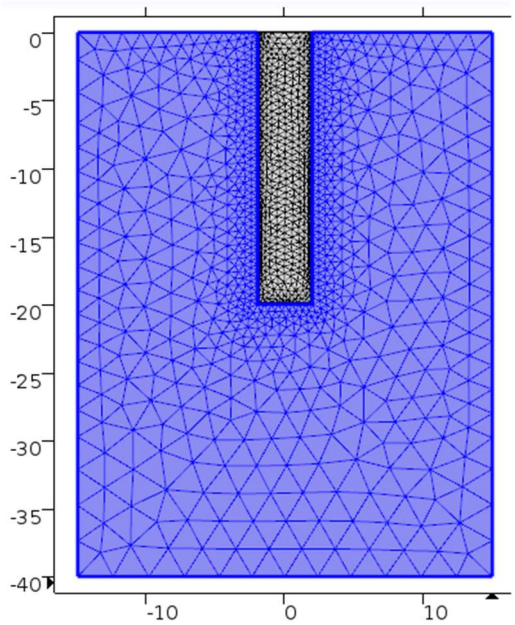

Figure 21. Mesh distribution

Cavity thickness [mm]	Water Initial Temperature [°C]	Mould Initial Temperature [°C]	Coolant Inlet Temperature [°C]	Fluid Velocity $[m/s]$	Ice Final Temperature [°C]
Ranging 1 to 5	8	-20	-20	0.25	-5

Table 8. Initial conditions

Element Size Parameters [mm]	Zone in blue (copper)	Zone in white (liquid)
Maximum element size	2.68	0.5
Minimum element size	0.012	0.012
Maximum element growth rate	1.3	1.1
Curvature factor	0.3	0.25
Boundary Layer	-	6 layers

Table 9. Mesh scale parameters

Experiment data does correlate with the simulated data as seen in Figure 22. According to AD-8495 amplifier[16] with the use of XF-1152-FAR K type thermocouple, it is specified in the datasheet that between -25 ºC and 400 ºC measurement temperature range, the maximum error on temperature readings is ±2ºC. Moreover, the computation outcome shows a slight fluctuation on 0ºC level and the major reason for it is the setup called phase transition interval which is set to 1.5ºC by me. Adjusting the interval setup extra fine takes much longer computation time and it also loads extra work on computer. For both lines, the error margin is specified in Figure 22.

16

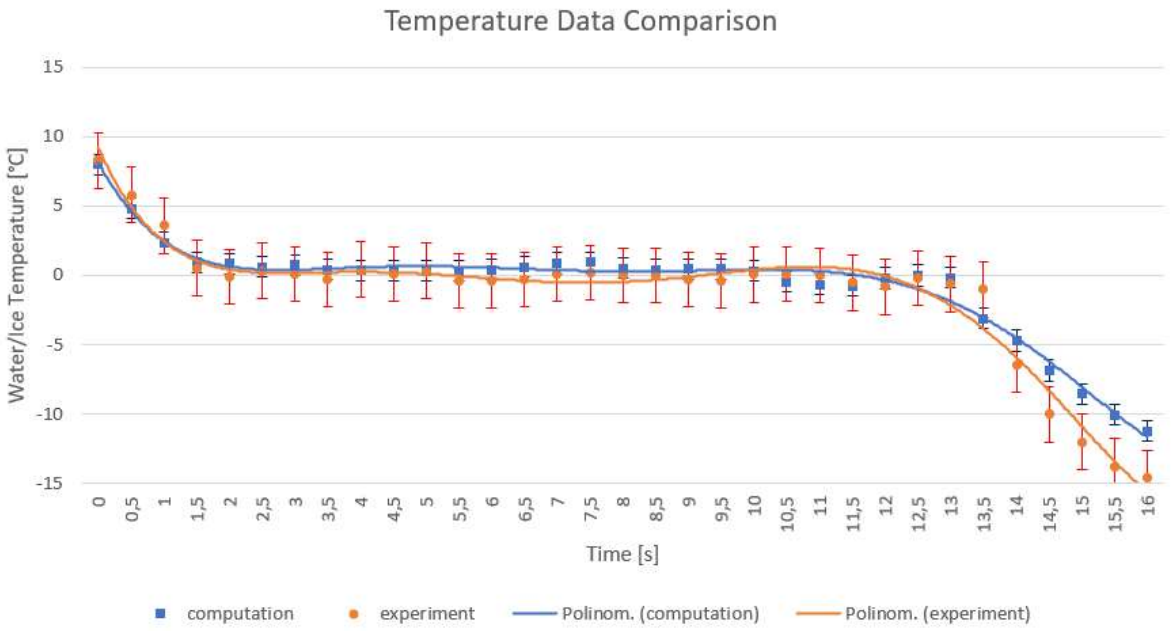

Figure 22. Defines the comparison between experimental and computational outcomes

Further simulations were performed in COMSOL Multiphysics in terms of optimum ice thickness in a specified time, ice survival time in a drink and how the ice reacts in a drink with distinct initial temperatures. Alcoholic drinks might be kept at various ambient conditions which is not ignorable.

Ice Thickness Sensitivity Study

In hypothesis, we have a limited time for ice formation which is about 10-15 seconds. With this constraint, the Figure 23 presents a wide insight on possible ice thicknesses with different mould temperatures. As mentioned in my design, one ice cube weighs 3.79 gram, the total energy to form 3 pieces of (-5°C) ice from (8°C) water is 4295 joules. The system can be cooled down to its initial temperature within 60 seconds. During the crystallization process ice cube expands with the rate of 1.087 against water volume.

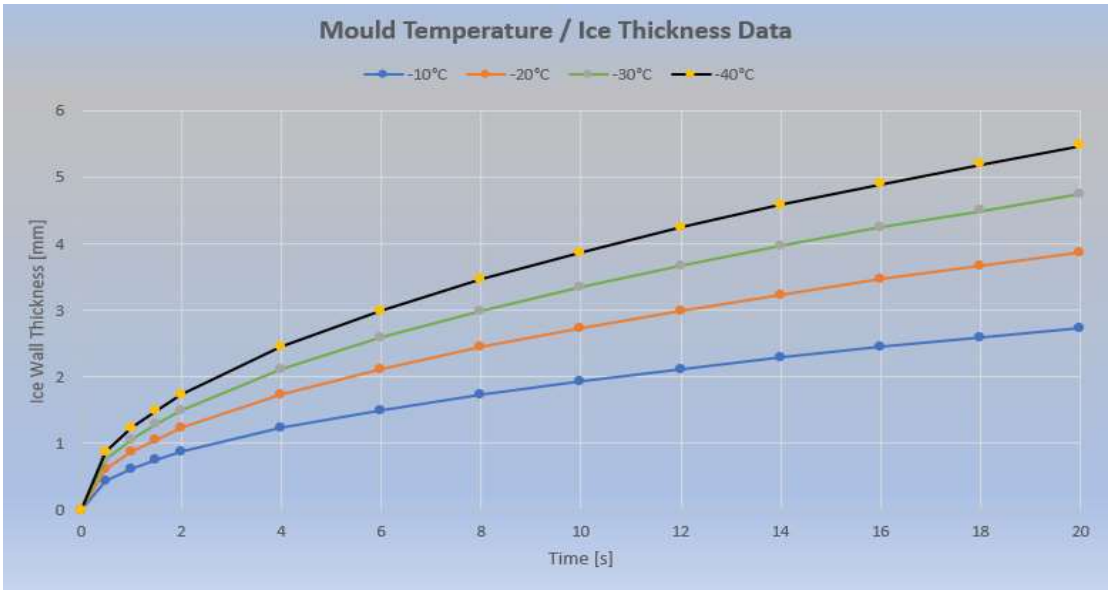

Figure 23. Ice thickness-Time Chart on different mould temperatures

Ice Effect On Hard and Soft Drinks

As demonstrated below in Figure 24, I computed cocktails with the different initial temperatures. The ice cubes initial temperature and the ambient air temperature are assumed to be -5°C and 25°C respectively. Furthermore, ice to drink ratio by volume inside glass is modelled 1:3 for hard drinks. On the other hand, the flat spot of each lines indicates the exact time when the ice cubes are fully melted in a drink. Afterwards, warmer environment conditions start to heat the drinks up gradually and over a couple of hours the drinks reach almost the ambient temperature.

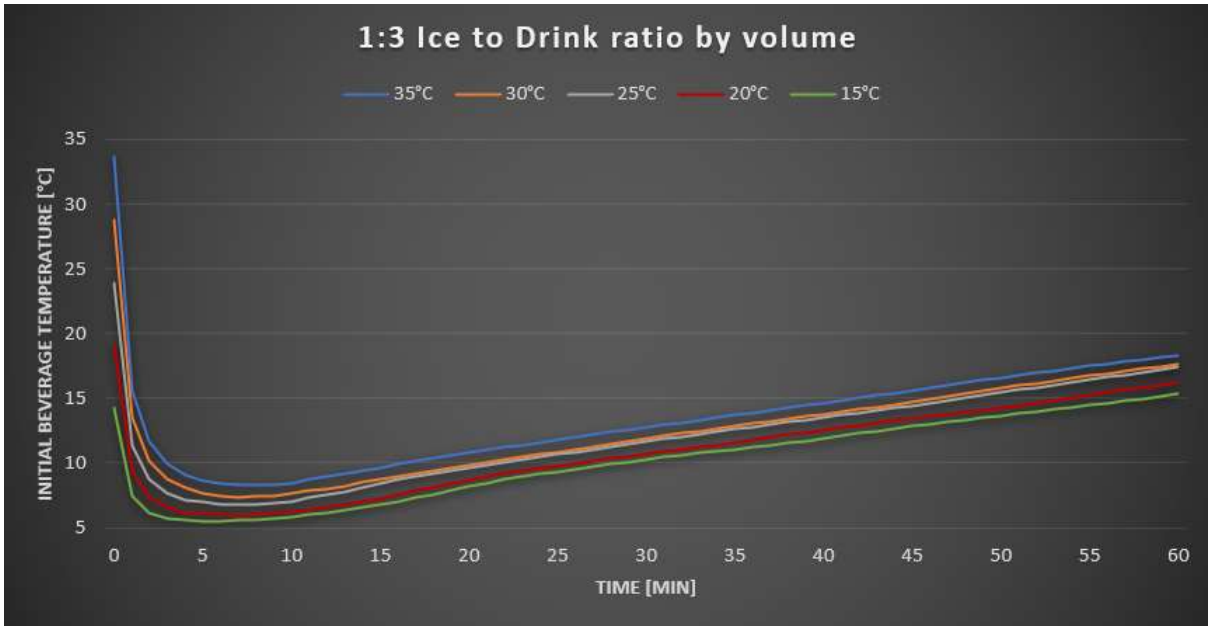

*Figure 24. Temperature gradient of a b*everage with the distinct initial temperatures with respect to time

In case a client would prefer a soft drink, it is assumed that 300ml of a glass shown in Figure 26, is filled by soft drink with dropping 3 ice cubes (12.36cc) inside. With this proportion, ice to drink ratio equals 1:25. The graph illustrated in Figure 25 has projected, a drink with ice content can be kept at its initial temperature about 30 minutes and gains only 2°C in an hour. Moreover, the drink temperature without ice rises 8°C in an hour. Overall, it is obvious that even if the ice content is quite low in a huge amount of drink, it has a considerable chilling impact.

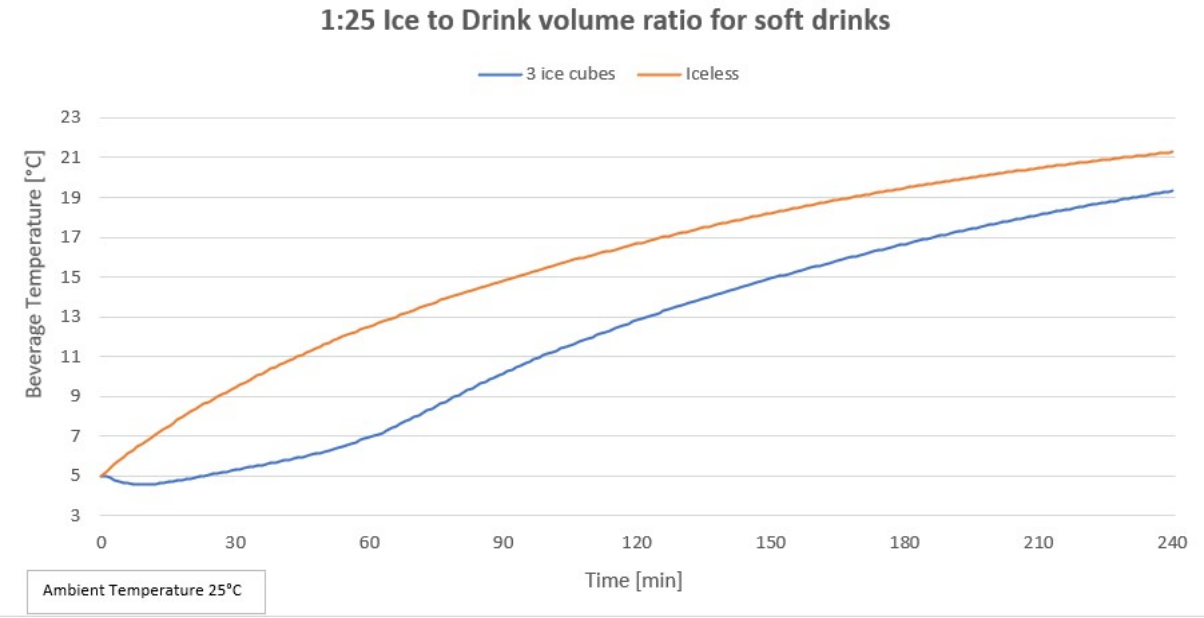

Figure 25. Graph demonstrates the beverage temperature gradient with ice cubes and without

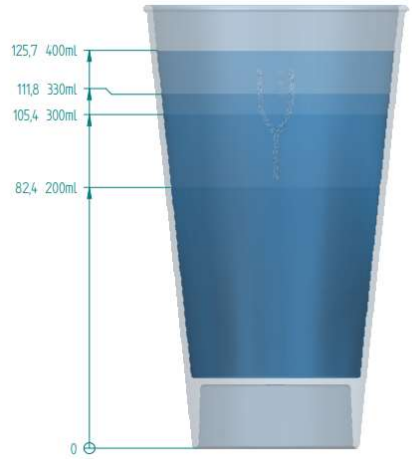

Figure 26. YANU highball glass made of polycarbonate (food grade)

5.CONCLUSION

Based on my research an ice machine that satisfies the solution requirements can be produced under 2 different working principles. The first idea is to fabricate a special mould by 3D metal printing which has conformal cooling channels to catch the highest cooling efficiency. The second idea is to develop a metal tray which is welded to evaporator coils. Here I explain both ideas technically and perform an analysis about which idea is more logical to go through.

- **3D Printing mould with conformal cooling channels**

It works with supplying a controlled amount of water into cavity. In this sense the quantity and geometry of ice cubes are uniform, there is no necessity for dispensing system.

Parameters	*Technical Data*
Coolant temperature	-20°C
Coolant flow velocity	0.25 m/s
Coolant pressure drop through channel	0.12 bar
Evaporator Capacity	0.344 kW
Circulation Pump Power	0.037 kW
Ice Wall Thickness	0.003 m
Ice Forming Time	~15 sec
Cycle Time	60 sec
Cooling heat transfer coefficient	553 $W/m^2.°K$
Length of channel	0.85m
Diameter of channel	0.004m
Compressor Power	0.111kW
Estimated Heat Loss to surroundings	0.027kW (ambient 22°C)
Ice production rate	11.37g/min
Refrigerant type	R134a
Ice geometry and dimension	Y shaped / 32x26x12 mm
Refrigerant mass flow rate	0.00265 kg/s
Total power required	148W + water pump(neglected)
Safety Margin	10%

Table 10. Technical Data for channel-cooling system

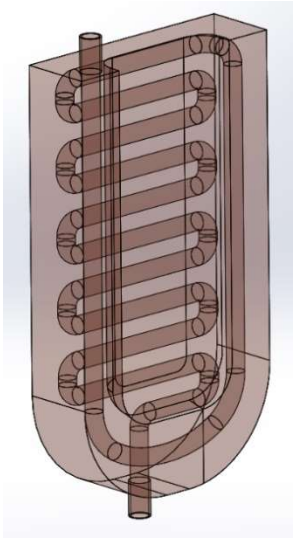

Figure 27. Conformal channels provide uniform cooling

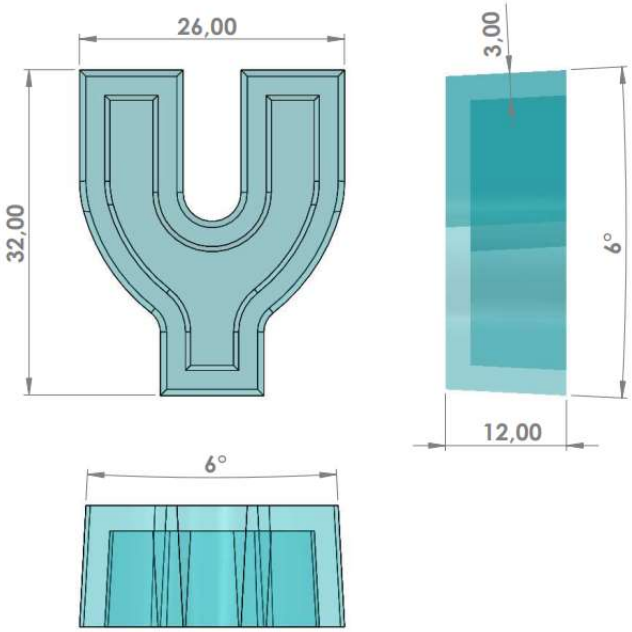

Figure 28. Ice piece technical drawing

The machine produces 3 ice cubes with the wall thickness of 3 mm, volume of 4120 mm^3 each and the ice cube shape has a 6° inward draft angle in both directions. The inner surface of the copper mould has been nickel plated which provides an extra smoothness for easier ice removal. The estimated cycle time is 60 seconds. The technical parameters above are determined by correlations which is widely stated in theoretical part. With a benefit of conformal channels, it enables mould to cool down uniformly their initial temperature within a minute.

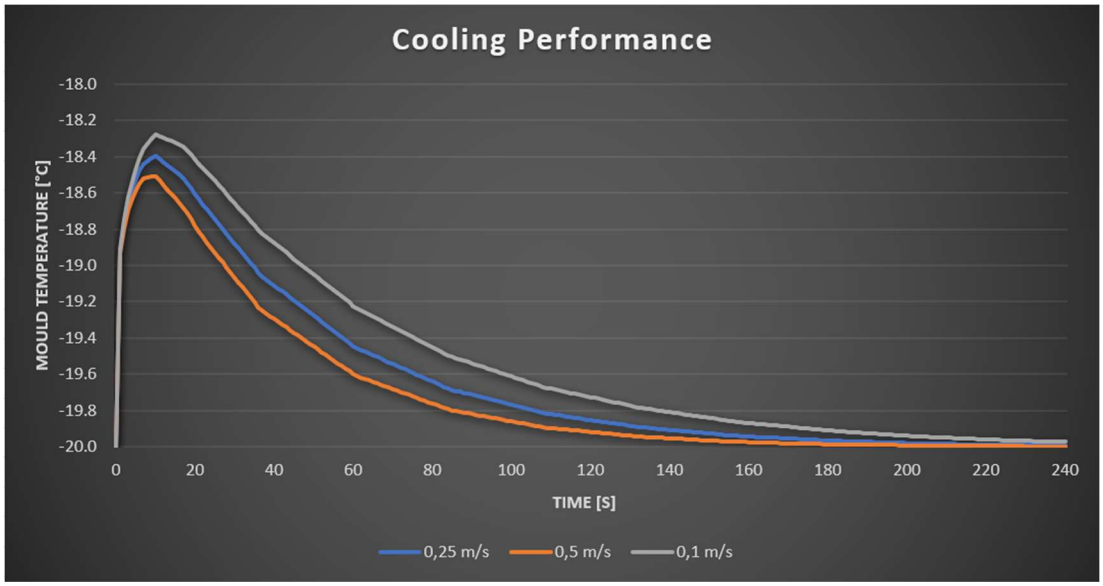

Figure 29. The chart points out the impact of the coolant flow velocity through mould block

The system is computed to figure out how long it takes to get back its initial temperature of -20°C. The cavity filled with 8°C water does heat the mould approximately 2°C, afterwards, the

dominance of circulation pays off. The higher coolant velocity provides rapid cooling performance but also requires powerful circulation pump.

- **A vertical copper tray welded on evaporator coils**

It works with supplying continuous water flow at the top of metal tray and first ice structures start forming on tray walls layer by layer until the desired thickness value has been formed. Afterwards the solenoid valve opens and enables to push hot refrigerant vapour(~47°C) through evaporator coils which generates an instant heating on tray. With this way ice cubes come out of tray and drops into the insulated ice bucket. To justify the amount of ice per cycle, a load cell is used which is a sensor measuring the ice cube mass. Otherwise misdispensing might happen due to nonuniform ice geometry.

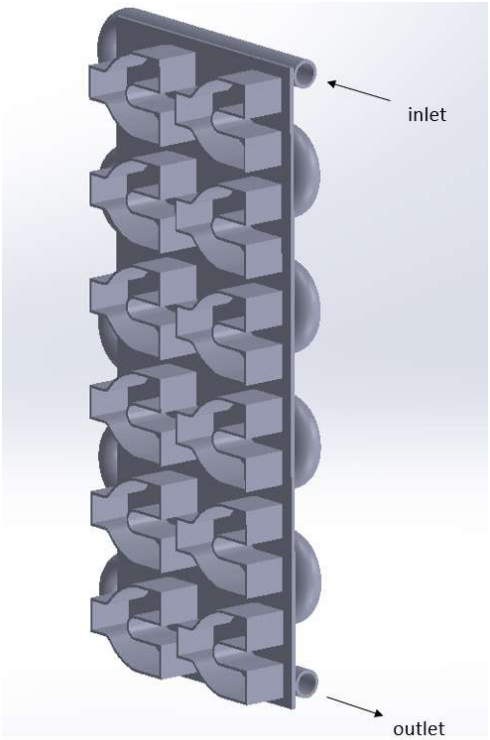

Figure 30. Tray grid where ice forms

Parameters	*Technical Data*
Evaporator Capacity	0.11kW
Cycle Time	13 min (for 3mm ice wall)
Compressor Power	0.035kW
Estimated Heat Loss to surroundings	0.027kW (22°C ambient)
Ice production rate	11.66g/min
Refrigerant Type	R134a
Evaporating Temperature	-20°C
Condensing Temperature	40°C
Evaporating Pressure	1.4 bar
Refrigeration effect	130 kJ/kg
Compression capacity	42 kJ/kg
Ice cube dimension	32x26x12 mm
Refrigerant mass flow rate	0.001 kg/s
Tray	40 cores
Total power required	35 W + water pump(neglected)

Safety Margin	10%

Table 11. Technical Data for Tray system

Below all elements needed for ice machine are expressed in Table 12.

ELEMENTS	Conformal cooling channel design	Tray welded on evaporator coils
Cooling liquid	Ethy. glycol aqueous solution 50%	-
Circulation pump for coolant	+	-
Coolant tank	+	-
Water reservoir	+	+
Water feeding pump	+	+
Condenser unit	+	+
Evaporator unit	+	+
Compressor unit	+	+
Expansion valve	+	+
Defrosting system	-	+
Refrigerant type	R134a	R134a
Precise Ice Dispensing	+	-
Insulated Ice Bucket	-	+
Working Principle	Precise water injection in cavity	Water flowing over tray

Table 12. System Components on both systems

5.1 TECHNICAL ANALYSIS BETWEEN BOTH PRINCIPLES

In market, majority of commercial ice machines cost in the range of 150-700$ with full units included. However, only the fabrication of 3D printed mould requires 5.000 to 10.000$ depending on the part size. Mainly that is because of metal powder cost. Furthermore, 95% of metal printed components are supposed to have additional post processing steps such as sintering, heat treatment. This idea comes along with circulation pump, coolant reservoir and tubing system connections. Based on 3D printed mould design, a circulation pump is necessary with a power of 0.037 kW. In addition, the machine should have a thermally insulated reservoir to keep the cooling fluid chill which causes an extra volume. Another drawback of the system is maintenance. In case the cooling channels are blocked for some reason, it might be challenging to clear through, especially if the path is not straight. For joints, Buna N tubing[17] material is needed, which is synthetic rubber, does have a flexible structure even at low temperatures like -20°C. Evacuation of ice might be difficult as this system has no instant heating impulse, although, draft angle design would have a benefit.

The positive side for this system is that no need for dispensing system, due to the fact that, a mould consisting 3 cavities is ready to serve 3 ice cubes on each cycle. Conformal cooling channels have provided optimum cooling performance. Whatever geometry the core has, these channels are positioned at a constant distance from ice forming walls all around.

Overall, scanning from the engineering perspective, both systems have nearly same ice production speed, 11g/min. The idea with cooling channels requires 113W extra power, plus the manufacturing cost between both systems cannot be underestimated. It occupies larger

17

space due to the coolant reservoir. Thereby, I would recommend to use the tray system as this idea is cost effective, energy saving and reliable to run for YANU.

List of Components for Preferred Ice Machine

1. Compressor
2. Solenoid valve for hot gas
3. Condenser
4. Condenser fan
5. Evaporator coils
6. Throttle (expansion valve)
7. Water pump
8. Insulated ice cube basket
9. Lines
10. Load cell
11. Dispensing mechanism
12. Bodyframe
13. Water filter
14. 34 core-nickel plated tray made of copper
15. Control unit
16. Temperature sensor

Acknowledgements

I would like to express my appreciation to my supervisor Alvo Aabloo for his mentoring and phenomenal contributions throughout this work. I am delighted to have our friendly chats and meetings every week. I appreciate YANU OÜ for supporting me in this period.

REFERENCES

[1] *Flippy 2*. Miso Robotics. (2022, May 21). Retrieved May 21, 2022, from https://misorobotics.com/flippy-2/

[2] *Cecilia - the first interactive bartender*. Cecilia.ai. (n.d.). Retrieved February 18, 2022, from https://cecilia.ai/

[3] *Milkit Dual Milk Tap System*. United Supplies. (n.d.). Retrieved March 18, 2022, from https://unitedsupplies.com.au/shop/category/milk-tap-system/milkit-dual-milk-tap/#collapse-additional_information

[4] *Catch up if you can*. Makr Shakr. (n.d.). Retrieved May 18, 2022, from https://www.makrshakr.com/

[5] *World's first contactless robot bar*. Yanu. (n.d.). Retrieved March 18, 2022, from https://yanu.ai/

[6] *Appendix B - log P/H diagrams for refrigerants*. SWEP. (n.d.). Retrieved March 18, 2022, from https://www.swep.net/refrigerant-handbook/appendix/appendix-b/

[7] *Arma*. (n.d.). Retrieved March 14, 2022, from https://www.arma.org.au/wp-content/uploads/2017/03/fundamentals-of-refrigeration-thermodynamics.pdf

[8] Cengel, Y. A. (2003). *Heat transfer: A practical approach*. McGraw-Hill.

[9] *File:Moody diagram.jpg - Wikimedia Commons*. (n.d.). Retrieved May 21, 2022, from https://commons.wikimedia.org/wiki/File:Moody_diagram.jpg

[10] *What is labview? Graphical Programming for Test & Measurement*. NI. (n.d.). Retrieved May 12, 2022, from https://www.ni.com/en-us/shop/labview.html

[11] Engineering, O. (2020, July 7). *Thermocouple response time*. https://www.omega.com/en-us/. Retrieved June 5, 2022, from https://www.omega.com/en-us/resources/thermocouples-response-time

[12] *What is a PT100 sensor working principle? sensors UK manufactured*. Process Parameters Ltd. (2022, May 9). Retrieved August 10, 2022, from https://www.processparameters.co.uk/pt100-sensor-working-principle/

[13] *Lauda® lck 1891 proline RP 1845 stainless steel refrigerated circulating water bath with master thermostat control, range: -50 to 200°C, bath volume: 12.5 to 19L, 230V/50Hz*. Capitol Scientific. (n.d.). Retrieved August 10, 2022, from https://www.capitolscientific.com/LAUDA-LCK-1891-Proline-RP-1845-Stainless-Steel-Refrigerated-Circulator-Bath-with-Master-Thermostat

[14] Paveldev. (n.d.). *Jahutusvedelik -36°C roheline*. Eesti suurim tööstuskemikaalide tarnija. Kemikaalide müük. Retrieved May 20, 2022, from https://masterchem.ee/toode/jahutusvedelik-36-c-roheline/

[15] *Multiphysics Cyclopedia*. COMSOL. (n.d.). Retrieved May 21, 2022, from https://www.comsol.com/multiphysics/heat-transfer-conservation-of-energy?parent=fluid-flow-heat-transfer-and-mass-transport-0402-442

[16] Reem Malik Download PDF. (n.d.). *1087: Thermocouple linearization when using the AD8494/AD8495/AD8496/AD8497*. AN. Retrieved August 10, 2022, from https://www.analog.com/en/app-notes/an-1087.html

[17] *Tubing & fittings guide - polyscience*. (n.d.). Retrieved July 10, 2022, from https://www.polyscience.com/sites/default/files/public/pdf/_selection-guides/Tubings&FittingsGuide.pdf

Appendix

Licence

Non-exclusive licence to reproduce thesis and make thesis public
I, Yigit Orhan

1. herewith grant the University of Tartu a free permit (non-exclusive licence) to reproduce, for the purpose of preservation, including for adding to the DSpace digital archives until the expiry of the term of copyright,

Rapid ice cube production with 3D printed copper moulds,

supervised by Alvo Aabloo.

2. I grant the University of Tartu a permit to make the work specified in p. 1 available to the public via the web environment of the University of Tartu, including via the DSpace digital archives, under the Creative Commons licence CC BY NC ND 3.0, which allows, by giving appropriate credit to the author, to reproduce, distribute the work and communicate it to the public, and prohibits the creation of derivative works and any commercial use of the work until the expiry of the term of copyright.

3. I am aware of the fact that the author retains the rights specified in p. 1 and 2.

1. I certify that granting the non-exclusive licence does not infringe other persons' intellectual property rights or rights arising from the personal data protection legislation.

Yigit Orhan

14/8/2022